RESEARCH ARTICLE

Solutions to Enhance Frequency Regulation in an Island System With Pumped-Hydro Storage Under 100% Renewable Energy Penetration

APOSTOLOS G. PAPAKONSTANTINOU[ID], **(Member, IEEE), APOSTOLOS I. KONSTANTEAS,
AND STAVROS A. PAPATHANASSIOU**[ID]**, (Senior Member, IEEE)**

School of Electrical and Computer Engineering, National Technical University of Athens (NTUA), 15773 Athens, Greece

Corresponding author: Apostolos G. Papakonstantinou (apopapak@central.ntua.gr)

ABSTRACT Seeking 100% renewable energy source (RES) penetration in low-inertia, isolated grids presents major challenges, including frequency control and stability. This is the case in small island systems relying on variable RES and pumped-hydro storage, where the limited ramping capabilities of hydro turbines compromise their frequency response. In this study, solutions are examined to allow the operation of such systems under 100% RES conditions. The Greek island of Ikaria is used as a study case, supplied by a hybrid RES-storage facility, consisting of hydroelectric units, a pumping facility and a wind farm. Solutions under study include the implementation of deflector control to allow provision of fast reserves by the Pelton hydro turbines, primary reserves provision by the wind farm, the enhancement of the variable speed pump control to contribute to primary frequency regulation, and, at a further step, the installation of battery energy storage to provide fast response for effective frequency regulation. All solutions are comparatively assessed via simulation to demonstrate that the proposed deflector control allows effective frequency regulation, albeit at the detriment of energy efficiency, whereas the variable speed pumps may also contribute to primary regulation in case of contingencies. It is battery storage that would decisively enhance frequency control and security of operation, while also allowing for improved tracking of wind power variations in normal operation; best results are achieved when batteries are combined with the other supplementary regulation measures, allowing a reduced battery capacity.

INDEX TERMS Autonomous systems, batteries, energy storage, frequency control, hydroelectric power generation, pumped storage, wind power generation.

I. INTRODUCTION

The deployment of energy storage systems (ESS) is vital to support the clean energy transition of the power sector, by providing an array of services [1], [2], [3], [4], especially in islands, given the particularities and technical challenges faced by isolated grids under high renewable energy source (RES) penetration. Battery energy storage

The associate editor coordinating the review of this manuscript and approving it for publication was Pratyasa Bhui[ID].

systems (BESS) is the ESS technology currently presenting the greatest development [1], by providing a broad range of services [5], [6], [7], [8], [9], [10]. Nevertheless, pumped hydro storage (PHS), the most mature storage technology, meets best long duration storage needs, with high arbitrage capability and capacity value [11], both necessary attributes to achieve very high RES share in the energy mix. However, PHS development on island grids faces several challenges, related to geomorphological requirements, long-lasting licensing and construction periods and limited

response speed [12], [13], [14], [15], [16], [17]. The latter is a result of water inertia effects, posing major challenges on frequency regulation of PHS-based island grids.

Water inertia effects can be mitigated by increasing the cross section of the pipes, or by installing a surge tank near the hydro turbines. Another option providing superior power regulation capabilities is the installation of variable speed PHS facilities, usually achieved by doubly-fed induction machine topologies in both hydro turbines and pumps [12], [13], [14], [18], [19], [20], [21]. Wind power smoothing can also be achieved by variable speed PHS stations co-located [15], [21], or not [13], [20], with wind farms (WFs). However, variable speed operation, as well as changing major design parameters of PHS facilities are not feasible for already operating plants, and come at a significantly high investment cost [12], [14], [18], [22].

A relatively cost-effective PHS solution combines fixed and variable speed pumps (FSPs, VSPs) and fixed speed generators as separate units. Such a topology is evident in the hybrid power stations (HPS) of El Hierro and Ikaria island systems. References [23], [24], [25], [26], and [27] study the capability of a pumping facility to provide frequency regulation services under various 100% RES conditions in El Hierro island grid, proving such units to be a useful source of reserves. References [16] and [17] examine also the capability of VSPs to effectively track the power produced by a WF within a HPS premises. Although pumping facilities including VSPs can support frequency control of island grids, heavily relying on these assets leads to extensive connections and disconnections of pumps, significantly increasing their wear [23]. Another major limitation on frequency regulation services provided by VSPs comes from their narrow speed -and power- operating range [16], [17], [23]. This is clearly demonstrated in [25] when VSPs are the only source of fast reserves in El Hierro, thus additional fast-acting sources are necessary to support operation under 100% RES. Moreover, pumping facility-WF coordination issues when the former is tracking the production of the latter, requires further investigation, considering practical limitations such as the necessary time between pump switchings and time delays associated with the communication network between the two facilities, both neglected in previous research [16], [17].

The capability of wind turbines (WTs) to support frequency regulation in non-interconnected grids dominated by PHS is well-established in the literature [16], [17], [24], [25], [27], [28], [29]. However, providing upward reserves requires wind power curtailments, reducing energy efficiency [28], [29]. Forecast errors in the day-ahead scheduling process, as well as uncertainties of real-time wind power estimation under curtailments, both lead to increased reserve requirements to ensure safe operation [30]. Limited reserve provision (5-10% of rated power [28]) can be achieved without curtailments, by extracting the energy stored in the rotating masses of WTs. However, the duration of such service is very limited, after which the power injection is even less

than the pre-fault value, for rotational speed restoration purposes [25], [27], negatively affecting the frequency restoration process [27]. In addition, wind turbine reserves are available only under favorable wind conditions [27], [31], [32]. However, frequency regulation is needed in all instances, including when hydro turbines are the only units committed online for power supply, so additional non-stochastic fast reserve sources must be available. For the above-mentioned reasons, the results of [27] demonstrate superior VSPs' contribution to WTs' in sustaining higher frequency nadirs under contingencies. Moreover, in cases where the pumps track the power generated by WTs, [16], [17] mention regulating issues when having WTs providing frequency control services, without furtherly studying such combination.

Limited research is available in utilizing deflectors for frequency regulation. These components deflect the water jet away from Pelton turbine blades, mostly for overspeed protection. Supporting power regulation in underfrequency events is also technically feasible, by positioning deflectors slightly within the water stream, albeit at the expense of energy efficiency [33]. A non-linear hysteresis deflector control is proposed in [34] as an overspeed protection measure, in which the deflector is fully open under normal state and fully closed during overspeed conditions. Such a control scheme is not suitable for frequency regulation purposes, due to its discontinuous response (deflector fully open/closed). In [22] and [35], two deflector control schemes are described to manage overspeed of the Bradley Lake impulse turbines, in case of load rejections. The focus of both references lies on a stability study of a hydroelectric project, rather than addressing the frequency regulation problem of PHS-based island grids in the presence of RES. Moreover, underfrequency events are not addressed, nor any comparative analysis with other measures supporting frequency regulation.

The combination of PHS and a fast acting storage unit, e.g. flywheel or batteries, is quite attractive due to the complementarity of their characteristics, with the PHS delivering energy arbitrage and firm capacity [11], whilst the fast acting storage unit provides fast response of limited duration. Flywheels are able to support frequency regulation, either installed on the hydroelectric turbine shaft, increasing system inertia [17], or as stand-alone assets [24], [25], [26]. Although effective, flywheels have a very low discharge duration, making them inappropriate for prolonged reserve provision. For this reason, flywheels offer a narrow range of benefits to island grids. Reference [24], studying flywheels' contribution on frequency regulation of island grids mentions "replacing flywheels by another fast storage system as batteries or supercapacitors" as good for future research.

The deployment of batteries alongside PHS facilities, even at relatively small capacities, may reduce the number of start-stop operations of pumps and the associated ramp rates, decreasing the operation and maintenance cost [18]. The flexibility offered by such combined storage plants is best suited for isolated systems [18], where they would outperform

plants having only one of the two technologies, in terms of functionality, reliability, cost and RES integration potential [36]. To the best of the authors' knowledge there has been very limited research on (a) frequency regulation capabilities of PHS, WTs and BESS operating as a single entity, under 100% RES conditions in isolated grids, and (b) any synergies between BESS and pumps in tracking wind power fluctuations.

In this paper, solutions are explored to achieve operation at 100% RES penetration in island grids relying on wind power and pumped-hydro storage. The non-interconnected island system of Ikaria, in which a PHS-based hybrid station is operating since 2019, is used as a study case. To address PHS limitations in providing effective frequency regulation services for isolated systems, the following alternative options are evaluated and comparatively assessed:

- Deflectors of the hydro units, to provide fast over- and under-frequency response, via a needle-deflector control method introduced in this work.
- Variable speed pumps to perform supplementary frequency regulation, in parallel to wind power tracking.
- Batteries within the hybrid station, as a fast-response device to enhance frequency regulation and wind power variability tracking. For the latter purpose, a BESS-VSP-WF coordinating control scheme is introduced in this paper.
- Wind farm of the hybrid station providing upward/downward primary reserves.

In all cases, the integration of each option in the overall control and management system of the plant is given due attention. The effect of communication delays in data exchange between remote locations is also examined.

The novelty and contribution of the paper lies in the following principal areas: (a) introduction of a novel deflector control scheme tailored to the needs of isolated systems supplied by PHS facilities, (b) development of coordinated control for the battery, pump station and wind farm components of PHS-based hybrid stations, (c) comparative assessment and determination of synergies between non-fossil-based fast reserve resources suitable for a PHS-supplied island grid.

The paper is organized as follows. Ikaria island system is presented in Section II, while the models and controllers of all system components are described in Section III. Simulation results are included in Section IV, whereas the main outcomes of this work are summarized in Section V.

II. IKARIA ISLAND SYSTEM

Ikaria is located in the Aegean Sea and has the highest RES share (~32%) amongst all non-interconnected islands of Greece, with a yearly load demand of ~28 GWh, and a peak-load of ~10 MW [37]. A PHS-based hybrid station is operating in the island since 2019. In Greece, the regulatory framework of hybrid power stations [38] has been introduced, as a means to increase RES penetration in its 28 non-interconnected island systems. Hybrid stations consist
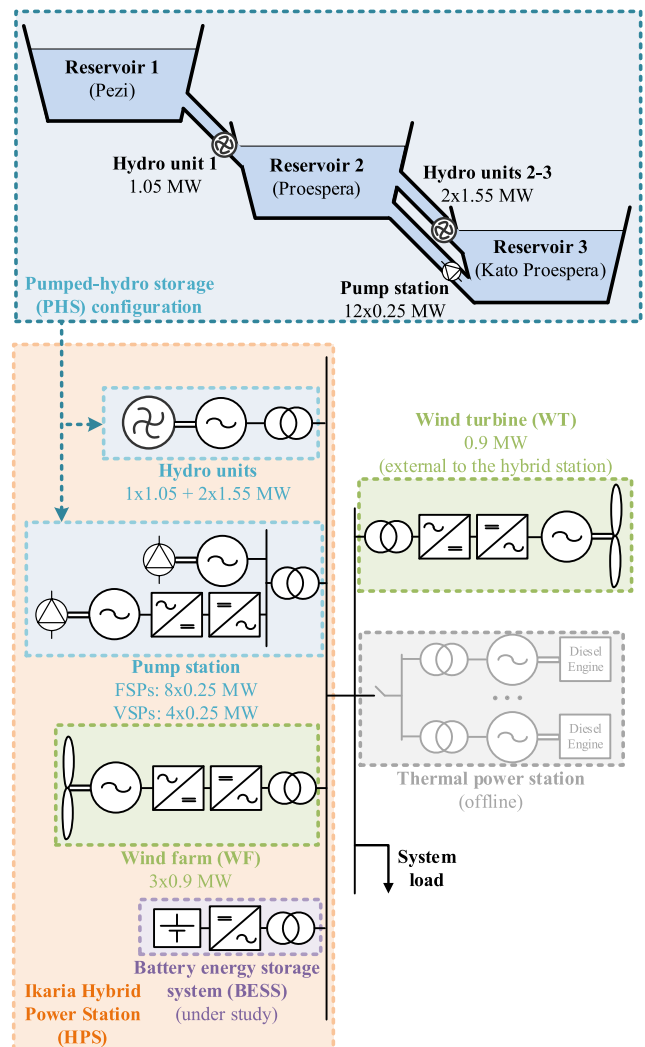

FIGURE 1. Ikaria island system.

of RES and storage units, operated in a coordinated manner to appear as a single dispatchable generating plant [39]. Available literature on the topic encompasses the optimum sizing analysis [40], [41], as well as scheduling and operating policy issues [39], [42], [43].

The island grid is shown in Fig. 1. The hybrid power station consists of three hydroelectric units (H1: 1.05 MW + H2-3: 2×1.55 MW), all equipped with Pelton turbines, a pumping station with 8 fixed speed and 4 variable speed pumps of 0.25 MW each and a 3×0.9 MW wind farm. Currently, the pumping station is controlled to track the output of the WF, compensating wind power variations that may disrupt frequency control. The latter has been provided by diesel units, which need to be replaced by hydro turbines if a high RES penetration is to be achieved. This, however, introduces significant challenges for frequency regulation, due to the slow response of hydroelectric units, because of water column inertia and the absence of a surge tank near the turbines. As a result, diesel units have to be maintained on-line by
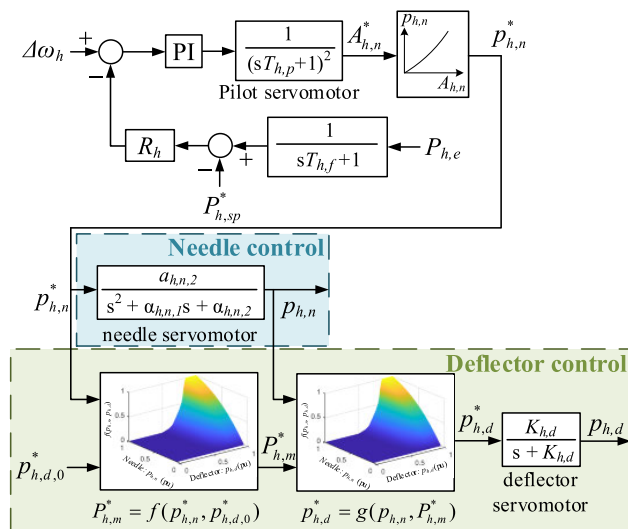
the system operator, severely impacting the achievable annual RES share.

The hybrid station has three (3) water reservoirs at different altitudes, as shown in Fig. 1. The pumping station installed at the base reservoir (Reservoir 3 at Kato Proespera) utilizes available wind energy to pump water from Reservoir 3 to Reservoir 2 (at Proespera). Both Reservoirs 2 and 3 have a capacity of roughly 80,000 m^3, each. The upper hydroelectric plant (unit H1) exploits water overflows from the 900,000 m^3 reservoir at Pezi (Reservoir 1), pre-existing for water supply and irrigation services, while the lower hydro plant (units H2-3) operates both on pumped water from Reservoir 3 and on overflows from Reservoir 1. Independent hydro turbine and pump penstock between Reservoirs 2 and 3 enable the simultaneous operation of generation and pump units.

The installation of a BESS within the hybrid station premises is also examined, to support the primary reserves provision, as well as the wind-power-tracking control scheme of the VSPs, as further explained in the following section. The thermal power station of the island is offline in the 100% RES conditions studied in this work. The island system also includes a single 0.9 MW WT, external to the hybrid station.

III. MODELS AND CONTROLLERS

A. WIND TURBINES

For the wind turbines, a typical full power converter model with a single-inertia representation of the drive train is used [44], [45]. The machine side converter (MSC) controller performs the maximum power point tracking (MPPT), by regulating rotor speed to its optimum value. A static optimum power–speed curve is used to calculate the speed reference from the measured WT power output. The current references of the controller responsible for tracking the electromagnetic torque reference are formed implementing a zero d-axis current control, to minimize losses in the generator and converter. The converter current control scheme is ensuring efficient current reference tracking via two PI controllers and the necessary decoupling terms. Further details on MSC control used can be found on [46], [47], and [48]. The pitch controller ensures that the active power does not exceed WT rated, via a PI controller [49].

In addition to maximum power point tracking assumed in most cases studied in this work (Section IV-A, B, D) wind farm's contribution to frequency regulation is also examined in Section IV-C. In such scenarios, the power reference (P_w^*) is formed as the superposition of a pre-defined percentage $(1 - r_w^*, r_w^*$: reserve margin) of the maximum available power ($P_{w,max}$), also known as "delta control" [32], and a droop control term to provide primary frequency regulation (R_w :droop coefficient), as noted in (1). Under curtailments, a simplified WT modeling is implemented, neglecting control issues evident in such conditions, e.g. wind power estimation errors and effective/stable coordinated rotor speed/pitch regulation ensuring the required reserve margin [31], [32], [50]. In all cases, the grid side converter (GSC) ensures that

FIGURE 2. Model used for the mechanical power of hydroelectric units.

the active power injected into the DC link by the MSC is transferred to the grid, through regulation of the DC link voltage [51].

$$P_w^* = (1 - r_w^*)P_{w,max} - \frac{1}{R_w}\Delta f \tag{1}$$

B. HYDROELECTRIC UNITS

1) MODEL OF HYDRAULIC TURBINES

The hydroelectric unit of Proespera (H1) is simulated using the elastic model described by (2), (3), (4) and (5), also shown in Fig. 2, which is explained in [52] and [53]. Kato Proespera turbines supplied through a common pipe (H2, H3) are simulated using a similar model, taking also into account the coupling effect between the individual unit penstock and the common pipe. The three-dimensional non-linear function $f(p_n, p_d)$ models the turbine mechanical power change with respect to the needle, p_n and deflector, p_d, positions, as analytically described in [35]. A power curve similar to that in [35] was developed to simulate the effect of p_n and p_d, as illustrated in Fig. 2.

$$A_{h,n} = k_{h,1}p_{h,n} + k_{h,2}p_{h,n}^2 \tag{2}$$
$$q_h = A_{h,n}\sqrt{h_h} \tag{3}$$
$$h_h = 1 - f_h q_h^2 - Z_{h,0}\tanh(sT_{h,e})q_h \tag{4}$$
$$P_{h,m} = A_{h,t}h_h(q_h - q_{h,nl})f(p_{h,n}, p_{h,d}) - A_{h,n}D_h\Delta\omega_h \tag{5}$$

2) PROPOSED ACTIVE POWER CONTROLLER

Pelton turbines use both needles and deflectors to regulate the amount of water discharged at the rotor blades and thus the mechanical power produced. The needles adjust the water flowing in the penstock, while the typical usage of the deflectors is to rapidly deflect water away from the turbine blades, to provide overspeed protection [34]. Power regulation is normally performed by adjusting the needle position ($p_{h,n}$). Due to water column dynamics, hydro units face limitations as regards the effective provision of fast reserves. For this reason, the possibility of utilizing the deflectors (position: $p_{h,d}$) for such services is also explored in this work.

Since deflector operation does not alter the water flow in the conduits, but only whether the water jets impact the

FIGURE 3. Proposed active power controller for hydroelectric units.

turbine blades, their response is not limited by water column dynamics and can therefore be quite fast [33]. Deflectors are primarily used in cases of rotor overspeed, acting rapidly to partially divert the water stream from going into the turbine buckets. In this way, deflectors can reduce the mechanical power produced, even in less than 1 s [35]. Upward reserve provision can only be achieved by letting the deflectors permanently divert part of the water stream in normal operation, which enables them to rapidly increase the flow incident on the turbine blades when needed, albeit at the expense of energy efficiency.

The proposed needle and deflector position controller utilizing the deflectors' capabilities is illustrated in Fig. 3. In the standard scheme, excluding deflector control (green-shaded area), the rotational speed deviation signal ($\Delta\omega_h$) is sent to a PI controller with permanent droop feedback, whose output forms the total needle jet area reference ($A_{h,n}^*$), converted to the needle position reference ($p_{h,n}^*$) through (2) correlating the needle jet area and position [35]. The needle servomotor regulates position ($p_{h,n}$) at a slow rate, as imposed by the water hammer effect limitations [35]. The pilot servomotor is modelled using a 2nd order filter transfer function [52].

The deflector regulator consists of two successive three-dimensional functions ($f(p_n, p_d)$, $g(p_n, P_m)$). The first ($f(p_n, p_d)$) produces the mechanical power reference for the turbine output ($P_{h,m}^*$), taking into account the needle position reference ($p_{h,n}^*$) dictated by the PI controller and the steady state deflector position reference ($p_{h,d,0}^*$). Thus, $P_{h,m}^*$ is the PI command translated into mechanical power. The second static curve ($g(p_n, P_m)$) receiving this power command takes into account the actual needle position ($p_{h,n}$) to develop the deflector position reference ($p_{h,d}^*$). Function $g(p_n, P_m)$ utilizes the same curves as $f(p_n, p_d)$, thus no additional information is required for obtaining its values. A servomotor, modelled according to [34], is then driving the deflector to its reference position. The static curves utilized in the control

scheme can be obtained for any Pelton turbine from the manufacturer and, if necessary, verified via field tests.

The PI controller gains are tuned considering the time-domain system response -mainly frequency range, settling time, and penstock pressure deviations- under a major contingency, ensuring effective control in less severe conditions [33], [54]. The tuning process began by estimating the PI gains without deflector control, utilizing the equations described in [53]. To enhance the dynamic operating characteristics of the governor, its controller has separate PI gains for operation without and with deflector control, choosing higher gains in the second case [33], as indicated in Table 6. Further details on tuning the governor of a hydroelectric unit without and with deflector control can be found in [22], [33], [35], [53], and [55], respectively.

According to this power control scheme, any command for a change in hydro power is sent to the needles' servomotor to initiate a needle position change. Given the slow response of the needles, the deflector position takes into account the measured needle position and makes up for any deviation from the governor command. Thus, the deflectors act first and adjust their position for the mechanical power to reach its reference. At the same time, the needles slowly adjust their own position, while the deflectors maintain the mechanical power of the turbine equal to the reference. In the end, the needles reach their final position, and the deflectors return to their steady state reference value ($p_{h,d,0}^*$).

This control principle is effective for downward regulation, as the water is quickly deflected away from the turbine blades. However, if deflectors are normally set to their maximum (full water jet) position, this leaves no room for upward regulation. To achieve this via deflector control, the water stream needs to be partially deflected away from the turbine blades in the steady state, wasting available hydro energy. Such a strategy, even though apparently inefficient, may still make sense in a saturated island system, where high RES curtailments inevitably take place. Considering the particular characteristics of the study-case system, a conservative approach of maintaining a limited reserve margin up to 10% is adopted in Section IV, to evaluate potential benefits out of such a control practice.

C. PUMPING STATION AND BATTERY STORAGE
1) FIXED SPEED PUMPS
The asynchronous motors of FSPs are directly connected to the pumping station busbars, presenting no controllability, other than connection/disconnection from the grid. Their hydraulic model considers an elastic water column for the common pipe, while rigid water dynamics are used for the short-length pipes to all individual pumps. The model used is described in [56].

2) VARIABLE SPEED PUMPS
VSPs are connected to the grid via a standard AC/DC/AC electrical drive converter. The asynchronous machine current dynamics are modelled based on [51]. The MSC regulates
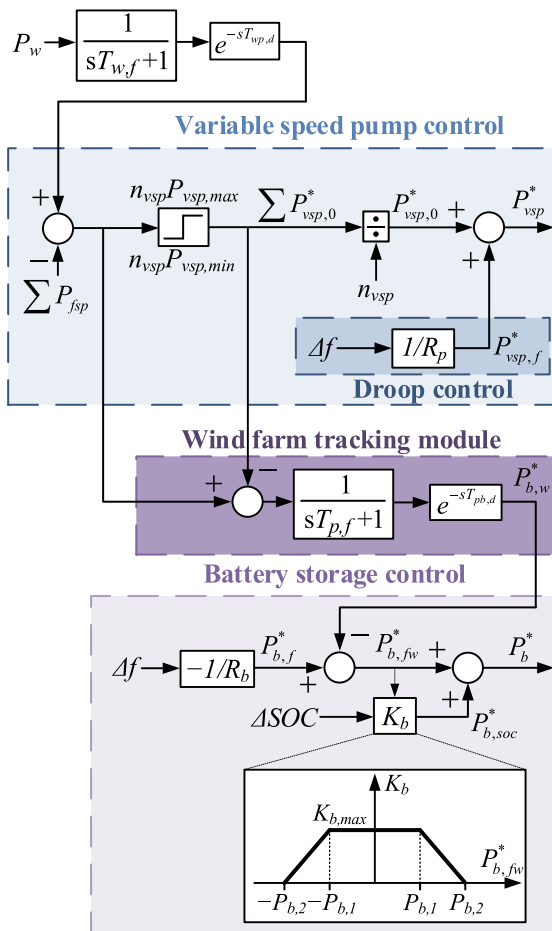
FIGURE 4. Variable speed pump and battery storage power controllers.

the power absorbed by the asynchronous motor, via torque control, while its flux is regulated to its nominal value. Torque and flux are controlled via the q- and d-axis stator currents, respectively, as in [51]. The control principle and model for the GSC is similar to the one used for the WT GSC.

To minimize the disturbances that may be caused to the grid by wind power fluctuations, the power absorbed by the pumping station closely tracks the wind power out of the WF. This is achieved by adjusting the power of the VSPs based on real-time measurements of the wind farm (P_w) and the FSPs' $\left(\sum P_{fsp} \right)$ power levels, as shown in Fig. 4. The WF production measurement filtering process (with time constant $T_{w,f}$) and the delay ($T_{wp,d}$) related to the WF-pumping station communication network, are also considered. In Ikaria HPS - as in most cases- the WF and the pumping facility are installed in different physical locations, so $T_{wp,d}$ is assumed equal to 1 s in the simulations presented in Section IV, which is a quite conservative assumption [57], [58].

In case of large wind power fluctuations, exceeding the VSP regulation margin, connection/disconnection of pumps may be effected, as explained in the following subsection. The total power reference for all VSPs, formed as the difference

between the measured wind and FSP power, is uniformly distributed to all operating VSPs (n_{vsp}).

Apart from tracking the available wind power, pumps may also provide primary frequency regulation via a droop-type command ($P_{vsp,f}^*$), if needed. The main parameters of the VSP control are included in the Appendix (Table 7).

3) PUMP MANAGEMENT PRINCIPLES
The FSP power can only be regulated stepwise, switching in and out individual pumps. VSPs may also have to be turned on/off in certain cases, to track large variations of the total pumping station power reference. A controller that determines the number of pumps in operation based on the power of the VSPs, similar to the one described in [23], is implemented. If the power of any operating VSP remains below a pre-defined minimum threshold (50% of rated), successive disconnection of FSPs takes place until underloading is resolved, observing a time delay between successive switchings ($T_{p,on/off} = 5$ s). VSPs may also be de-committed if needed. The same principle is applied when a VSP reaches its maximum power, to cut in additional FSPs.

4) BATTERY ENERGY STORAGE SYSTEM
The integration of a BESS in the hybrid station is also examined, to support frequency regulation and enhance the internal balancing of the station. The BESS provides primary frequency reserves through the droop control term (R_b: droop coefficient) in Fig. 4.

A WF tracking module shown in Fig. 4 is also introduced in some of the scenarios examined in Section IV. When the VSPs reach their regulation limits (operating range: $n_{vsp}P_{vsp,min} - n_{vsp}P_{vsp,max}$), the power deficit/surplus is fed to the BESS ($P_{b,w}^*$) to support wind-power-tracking, until the VSPs are restored to their operating range (through the start/stop of pumps). This control scheme requires a fast and reliable communication channel between the pumping facility and the BESS. Although co-locating these two systems would make sense, considering the modular form of battery systems, the resulting BESS connection cost reduction, and the minimization of any latency amongst those facilities, a conservative time delay of $T_{pb,d} = 1$ s [57], [58] is assumed in the communication channel between these units, to examine the control efficiency in the most challenging case of having these facilities located relatively far apart from each other.

The active power reference in steady state ($P_{b,soc}^*$) is performing battery energy reserves' regulation, via an adaptive proportional SOC controller. Its gain (K_b) is taking non-zero values only when the total active power required for frequency regulation and wind farm tracking purposes ($P_{b,fw}^*$) is within a narrow range ($\left| P_{b,fw}^* \right| < P_{b,2}$), as shown in Fig. 4. The same current controller as applied for the WT GSC is also used for the BESS. The Li-ion battery cells are simulated according to the model described in [59].

IV. SIMULATION RESULTS

This section presents the time-domain simulation results of Ikaria island system performed in MATLAB/Simulink, under 100% RES conditions. Studying the deflector control scheme, the operation with 0% and 10% reserve margins is examined. Primary frequency control enhancement by a 0.5 MW/0.5 MWh or 1 MW/1 MWh BESS, and the option of utilizing the VSPs' capability for primary frequency control are also explored. BESS operates under droop control in all scenarios, whereas in some cases the wind-farm-tracking module (*wft* in scenario notation), explained in the previous section, is also active.

All scenarios are evaluated against a so-called business-as-usual (*bau*) case: no BESS is used, the hydro units are controlled through their needle valves (no deflector control), VSPs are solely used for wind power tracking purposes, and no wind energy curtailments occur. Subsection A presents system response under high wind speed volatility, whereas Subsection B examines the grid operation in case of a contingency. In both subsections no wind power curtailments occur. The effectiveness of WF contribution to frequency regulation is explored in Subsection C. The importance of the time lag in the WF-pumping facility-BESS communication channel is examined in Subsection D. Subsection E includes a discussion based on the simulations results.

A. SYSTEM RESPONSE UNDER HIGHLY VARIABLE WIND CONDITIONS

In this section, grid operation is analyzed under highly variable wind conditions, with a 3.7 MW system load, without wind power curtailments. The effectiveness of different options is analyzed simulating the response of the Ikaria system for 30 scenarios, for the same high-turbulence 4-minute interval. The resulting key performance indices (KPIs), summarized in Table 1, reveal the effectiveness of each option. Three frequency quality metrics quantify the effect on system frequency regulation, namely the frequency range (f_{max}, f_{min}), standard deviation (σ_f) and time outside the 49.8-50.2 Hz window ($t_{out\pm0.2Hz}$). The response is characterized as "acceptable" when the frequency stays above 48.5 Hz (threshold for under-frequency load shedding activation) over the entire simulation period. The 4th KPI is the water quantity left unexploited for electricity generation ($q_{un-exploited}$), through deflector engagement. The last KPI is the energy throughput of batteries (ET_b) throughout the 4-minute period simulated, used as an indicator of BESS cycling and resulting wear.

For illustration purposes, the system response is presented in Fig. 5 for 4 scenarios examined, all including a 0.5-MW BESS in the hybrid station. In case (i) BESS is implementing droop control (*b0.5*), whereas in case (ii) the wind-farm-tracking module of the BESS is also active (*b0.5(wft)*). In case (iii) VSPs implement droop control (*b0.5+vsp*), in addition to tracking the WF power output. In case (iv) deflector control

is activated for all hydro units, with a 10% reserve margin (*b0.5+def10%*).

As seen in Table 1, frequency response in *bau* is clearly unacceptable, with the hydro units being unable to effectively contain frequency excursions, due to their low ramping capability imposed by the water column dynamics (max rate of change of needle position ∼2%/s). According to Table 1, in the absence of a BESS the frequency will always deviate lower than 48 Hz, indicating a compromised security of system operation.

A 0.5 MW BESS on droop control (*b0.5*) results in reduced frequency excursions. Yet, when the BESS output saturates at its maximum value (e.g., interval 200-220 s in Fig. 5) major under-frequency conditions are noted ($f < 48$ Hz). With a 1 MW BESS in droop control, frequency is contained in 48.9-50.6 Hz, even in the absence of any supplementary regulation measure. The SOC is varying near its reference value (55%) in all cases examined (Fig. 5 (h)), mainly due to the deployment of both upward and downward primary reserves, as shown in Fig. 5 (g). Thus, the severity of frequency regulation issues in the examined 4-minute period leaves little room for SOC control activation presented in Fig. 4.

Evaluating the KPIs in all scenarios, with and without the WF-tracking module, the proposed BESS-VSP-WF coordination scheme clearly enhances frequency response, as the batteries compensate any imbalance between pumping station and WF powers occurring when VSPs reach the operating limits (50-100%), before such imbalances are translated into frequency deviations. The effectiveness of the WFT control is greatly affected by BESS power capacity, since higher levels increase the regulation margin necessary to supplement the WFT performed by the pumping facility (e.g., average σ_f decrease when implementing WFT: 11% and 42% in cases with 0.5 MW and 1 MW BESS, respectively). However, the improved frequency quality metrics come at the cost of increased BESS wear (e.g. increase of average battery energy throughput by 19%). The zoom insets in Fig. 5 (e), (f), (g) show the WF-tracking activation in 72-84 s, where a large wind power decrease occurs, which the VSPs are unable to track, leading to an underfrequency event. With WF-tracking activated, BESS reaches its full power capacity (0.5 MW) at 76 s (against a 0.3 MW power output without WF-tracking), maintaining this power level for around 5 s.

Activating VSP droop control is beneficial for frequency response, but VSPs are unable to mitigate all power equilibrium disturbances taking place in the simulation interval. Large over/under-frequency events occur in periods of rapid wind power change, when the VSPs regulation range is already fully utilized by the wind power-tracking control. In such cases, similar KPIs are recorded in Table 1 with and without VSP droop control.

Deflector control, without maintaining upward reserves, is most effective in containing over-frequency events by rapidly reducing the output of the hydroelectric units. The frequency nadirs are also indirectly affected, due to the

TABLE 1. Key performance indices of scenarios examined at high wind volatility conditions: Frequency maximum (f_{max}), minimum (f_{min}) & standard deviation (σ_f), time outside the 49.8-50.2 Hz window ($t_{out\pm0.2Hz}$), un-exploited water flow ($q_{un-exploited}$) and battery energy throughput (ET_b).

No	Scenario	BESS rated power (MW)	Deflector reserve (%)	VSP droop control	BESS wind farm tracking	f_{max} (Hz)	f_{min} (Hz)	σ_f (Hz)	$t_{out\pm0.2Hz}$ (%)	$q_{un-exploited}$ (%)	ET_b (kWh)
1	*bau*	-	-	no	-	>52	<48	3.86	92	0	0
2	*vsp*	-	-	yes	-	>52	<48	1.96	83	0	0
3	*def0%*	-	0	no	-	51.7	<48	1.20	85	6.3	0
4	*vsp+def0%*	-	0	yes	-	51.7	<48	1.23	76	4.8	0
5	*def10%*	-	10	no	-	51.5	<48	0.94	75	11.5	0
6	*vsp+def10%*	-	10	yes	-	51.4	<48	0.84	73	10.7	0
7	*b0.5*	0.5	-	no	no	51.6	<48	0.84	65	0	14.5
8	*b0.5(wft)*	0.5	-	no	yes	51.4	<48	0.77	60	0	15.7
9	*b0.5+vsp*	0.5	-	yes	no	51.6	<48	0.79	58	0	13.3
10	*b0.5(wft)+vsp*	0.5	-	yes	yes	51.4	<48	0.75	53	0	13.5
11	*b0.5+def0%*	0.5	0	no	no	50.9	<48	0.58	64	4.1	12.1
12	*b0.5(wft) +def0%*	0.5	0	no	yes	50.8	<48	0.53	49	3.2	14.0
13	*b0.5+vsp+def0%*	0.5	0	yes	no	50.9	<48	0.54	63	3.3	11.1
14	*b0.5(wft)+vsp+def0%*	0.5	0	yes	yes	50.7	48.0	0.48	53	2.1	11.8
15	*b0.5+def10%*	0.5	10	no	no	50.7	48.8	0.40	51	10.6	9.3
16	*b0.5(wft)+def10%*	0.5	10	no	yes	50.5	48.9	0.32	35	10.3	12.9
17	*b0.5+vsp+def10%*	0.5	10	yes	no	50.7	48.9	0.36	40	10.4	8.4
18	*b0.5(wft)+vsp+def10%*	0.5	10	yes	yes	50.5	49.0	0.28	30	10.0	11.6
19	*b1*	1	-	no	no	50.6	49.0	0.38	48	0	18.6
20	*b1(wft)*	1	-	no	yes	50.3	49.2	0.23	32	0	20.7
21	*b1+vsp*	1	-	yes	no	50.6	49.0	0.37	45	0	17.8
22	*b1(wft)+vsp*	1	-	yes	yes	50.4	48.9	0.26	29	0	19.5
23	*b1+def0%*	1	0	no	no	50.5	49.1	0.32	40	3.0	15.2
24	*b1(wft)+def0%*	1	0	no	yes	50.3	49.4	0.18	19	1.5	18.0
25	*b1+vsp+def0%*	1	0	yes	no	50.5	49.1	0.30	31	2.1	14.1
26	*b1(wft)+vsp+def0%*	1	0	yes	yes	50.3	49.4	0.16	16	1.5	16.6
27	*b1+def10%*	1	10	no	no	50.5	49.3	0.26	35	9.9	12.6
28	*b1(wft)+def10%*	1	10	no	yes	50.2	49.5	0.13	13	10.0	17.6
29	*b1+vsp+def10%*	1	10	yes	no	50.4	49.3	0.25	31	10.0	11.7
30	*b1(wft)+vsp+def10%*	1	10	yes	yes	50.2	49.5	0.13	12	10.0	16.5

damping effect of deflector control in over-frequency time periods. Adopting a permanent deflector upward regulation margin of 10% (*def10%*) -i.e. a total active power reserve of ~0.3 MW by all three on-line hydro units- a significant improvement is noted (62% average σ_f reduction in all scenarios), with frequency excursions now remaining in the range 48.8-50.7 Hz in *b0.5+def10%*. This headroom for upward regulation comes at a cost of wasting ~10.3% of available water resource for electricity generation by unit H1 (see Table 1). The maximum frequency observed in scenarios with 10% reserve margin on hydroelectric units (*def10%*) is similar as in cases with *def0%*, since the hydro units' upward regulation margin has no direct effect on over-frequency events (average f_{max} difference 0.1 Hz, whereas average f_{min} difference is 0.7 Hz). An additional benefit of implementing a 10% reserve margin for hydro units is the reduced BESS energy throughput (25% reduction in all scenarios).

Fig. 5 shows in more detail the active power (Fig. 5 (b)), needle position (Fig. 5 (c)) and deflector position (Fig. 5 (d)) of the single hydro unit located in Proespera (H1: 1.05 MW). In all scenarios not having deflector control, the unit is participating in frequency regulation only through needle control, as shown in Fig. 5 (b), (c), which is clearly insufficient to provide effective regulation. When operating with a 10% upward

regulation margin, the deflector position fluctuates around a value below maximum (Fig. 5 (d)), providing fast upward regulation when needed. The deflector position reaches its maximum in significant under-frequency events (50-60 s, 205-215 s). To have the same active power injected to the grid in all scenarios examined, the needle position is higher when operating with deflector reserves, as shown in Fig. 5 (c), to compensate deflector losses. As seen in Fig. 5 (c), (d), the fast needle reference changes produced by the PI regulator of Fig. 3 are taken up by the deflector controller, with the needle position following these changes at a much slower pace.

Fig. 5 (e) depicts the active power absorbed by the pumps, along with the power produced by the WF of the hybrid station (in green solid line, same in all scenarios). The number of on-line pumps is shown in Fig. 5 (f). In periods with mild wind power variations (e.g., 130-140, 180-190 s), the pumping station manages to track wind power fluctuations (Fig. 5 (e)), not allowing any substantial imbalance to cause frequency deviations (Fig. 5 (a)). However, the wind-power-following control scheme implemented by the pumping station is unable to fully track wind turbine output under highly varying wind speed conditions, mainly due to the minimum time limitation of 5 s between start-stops of pumps. This is a critical parameter in the design of the pump
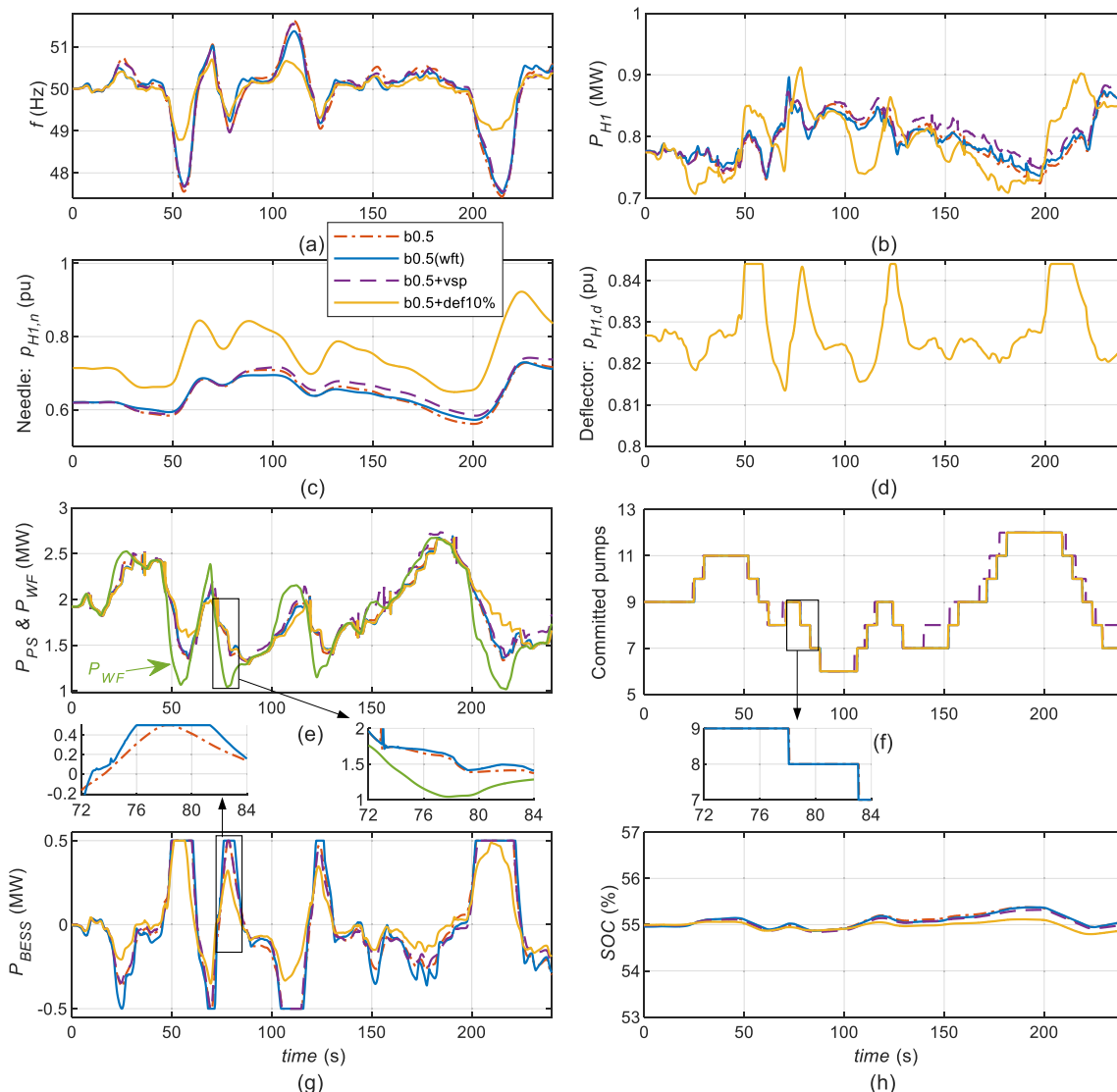
FIGURE 5. System response under high wind fluctuation conditions for 4 scenarios with a 0.5 MW BESS. (a) Frequency, (b) hydroelectric unit 1 (H1) active power, (c) H1 needle position, (d) H1 deflector position, (e) pumping station and wind farm active power, (f) number of pumps committed, (g) BESS active power, (h) BESS state of charge.

facility, indicating an important trade-off between operation and maintenance cost and accurate wind-power tracking performance. Another important factor is the latency in the data exchange between the WF and the pumping station, as explained in Subsection D.

Evaluating the results of all examined scenarios, the frequency stays above the 48.5 Hz limit when using a 0.5 MW BESS only if it is combined with a 10% reserve margin in the hydro units through permanent deflector activation, which comes at a cost of not exploiting an equivalent amount of the water for electricity generation. This inefficiency needs to be further evaluated taking account of the level of curtailment that inevitable takes place in an autonomous system operating at high RES penetration levels. A 1 MW BESS leads to acceptable response in all cases, with deflector and/or WF-tracking control again contributing to system stability. Overall, BESS is clearly the most effective solution

to ensure frequency regulation at 100% RES conditions; the WF-tracking module contributes to balancing wind power variations before they disturb frequency regulation of the system, while the proposed deflector control is a supplementary solution to enhance the capability of hydro units to provide fast reserves and reduce the BESS wear.

B. SYSTEM RESPONSE FOLLOWING A GENERATOR OUTAGE

In this section, the response of the island grid is examined following the sudden loss of a hydro unit located in Kato Proespera (H3) producing ~0.9 MW (30% of the 3-MW system load). The wind speed is assumed constant over the 1-minute simulation interval. The generator trips at $t = 10$ s and the minimum frequency reached after the disturbance is shown in Table 2. The activation of the wind-farm-tracking module in the BESS controller (Fig. 4) makes no difference

TABLE 2. Minimum frequency (f_{min}) of scenarios examined following a hydroelectric unit (H3) tripping.

No	Scenario	BESS rated power (MW)	Deflector reserve (%)	VSP droop control	f_{min} (Hz)
1	bau	-	-	no	<48
2	vsp	-	-	yes	<48
3	def10%	-	10	no	<48
4	vsp+def10%	-	10	yes	48.1
5	b0.5	0.5	-	no	<48
6	b0.5+vsp	0.5	-	yes	49.1
7	b0.5+def10%	0.5	10	no	48.9
8	b0.5+vsp+def10%	0.5	10	yes	49.3
9	b1	1	-	no	49.3
10	b1+vsp	1	-	yes	49.5
11	b1+def10%	1	10	no	49.4
12	b1+vsp+def10%	1	10	yes	49.5

under these conditions, due to the fixed wind speed profile. Scenarios with active deflector control but no permanent reserves are also of no interest, as the contingency examined requires the deployment of upward reserves.

The lack of primary reserves leads to unacceptable under-frequency events in all scenarios without BESS. The deflectors' capability to prevent major underfrequencies is limited, due to the small reserve margin of ∼0.2 MW in the remaining two hydro units, which represents only a small fraction of lost generation output. The same holds when VSPs are on droop control, as their primary reserves are insufficient to contain the imbalance.

The system response is demonstrated in Fig. 6 for the same scenarios as in Subsection A (except b0.5(wft)). The unacceptable frequency response in bau is enhanced when installing a fast-acting energy storage unit, but the 0.5 MW BESS is insufficient to fully address system needs and maintain frequency above 48.5 Hz.

Activating the VSP droop control, leads to acceptable frequency nadir (49.1 Hz) even with the small BESS. The pumping facility provides upward reserves of ∼0.2 MW by decreasing its power just after the disturbance, as shown in Fig. 6 (e). The contribution of VSP droop control to frequency containment is significantly higher in the generator outage, in comparison to conditions with high wind fluctuations (Subsection A); in the latter case the wind power tracking functionality leaves significantly lower capacity margin for VSPs to contribute to frequency regulation. The pumping station's power variations noted in scenarios without VSP droop control are due to the frequency deviations, affecting the FSPs' power level. A negative effect of activating the wind-power-tracking scheme of the VSPs (shown in Fig. 4) without droop control is that under-frequency events lead to reduced P_{FSP}, and thus a power imbalance between the pumps and WF, which the VSPs cover by increasing their power absorption, while the system is facing a power deficit. For this reason, the VSPs' droop control is considered a

necessary attribute for the overall active power regulation scheme of the hybrid station.

When hydro units operate with deflector regulation reserves, these are deployed within 1 s following the under-frequency event, as seen in the zoom inset of Fig. 6 (d). The needle position remains practically constant in such a short time interval, as shown in Fig. 6 (c). Between 20-30 s, the frequency gradually returns to 50 Hz and the needle position increases towards a new (higher) steady state value, leading the deflectors to return to their pre-fault state. The minimum frequency level in b0.5+def10% (48.9 Hz) is acceptable and similar as for b0.5+vsp.

With the 1 MW BESS, the disturbance is effectively managed (f_{min} = 49.3 Hz). However, a 0.5 MW BESS combined with deflector control with a 10% reserve margin and droop control on VSPs also leads to acceptable frequency nadir. Thus, these solutions are valuable supplementary resources, which need to be taken into account when sizing the necessary BESS.

C. WIND FARM CONTRIBUTION TO FREQUENCY REGULATION

If curtailing RES energy for frequency regulation purposes is acceptable (deflector control), then it makes sense to also evaluate wind energy curtailments, as a means to allow the HPS WF to provide primary reserves. First, the conditions of Subsection A are considered, while curtailing 17% of available wind power.[1] The results for the scenarios studied are presented in Table 3, along with the respective scenarios without the WF supporting frequency control (deflector control activated), for comparison purposes. Indicative simulation results are shown in Fig. 7. Fig. 7 (b) presents WF output under MPPT (b0.5+def10%) and under curtailment for frequency regulation (b0.5+wf17%); the pump station absorbed power is also shown in the second case.

The WF may contribute to frequency regulation by switching to MPPT control in case of wind speed dips (e.g. 50-60 s, 200-230 s), and also by mitigating rapid wind power increases causing over-frequency events (e.g. 60-70 s, 105-115 s). However, WF frequency response is countered by the pumps, that continuously track wind power production in an attempt to compensate the effect of fast wind power variations for the system.[2] This is evident in 165-190 s ($f >$ 50.2 Hz), where WF operation keeps shifting away from its MPP to provide downward regulation, but this is partly canceled-out by the pumps. So, the WF contribution to frequency containment comes indirectly via smoothening wind power variations under severe wind speed fluctuations, not by

---

[1]A higher percentage is assumed for the WF (compared to 10% for the hydroelectric units) to obtain the same upward regulation margin in MW, given that the average WF production is lower than that of the three (3) hydroelectric units.

[2]A 1 s lag is evident due to the communication delay assumed to exist between the WF and the pump station. Time between consecutive pump switching (5 s) is another cause of real-time mismatch between the two facilities.
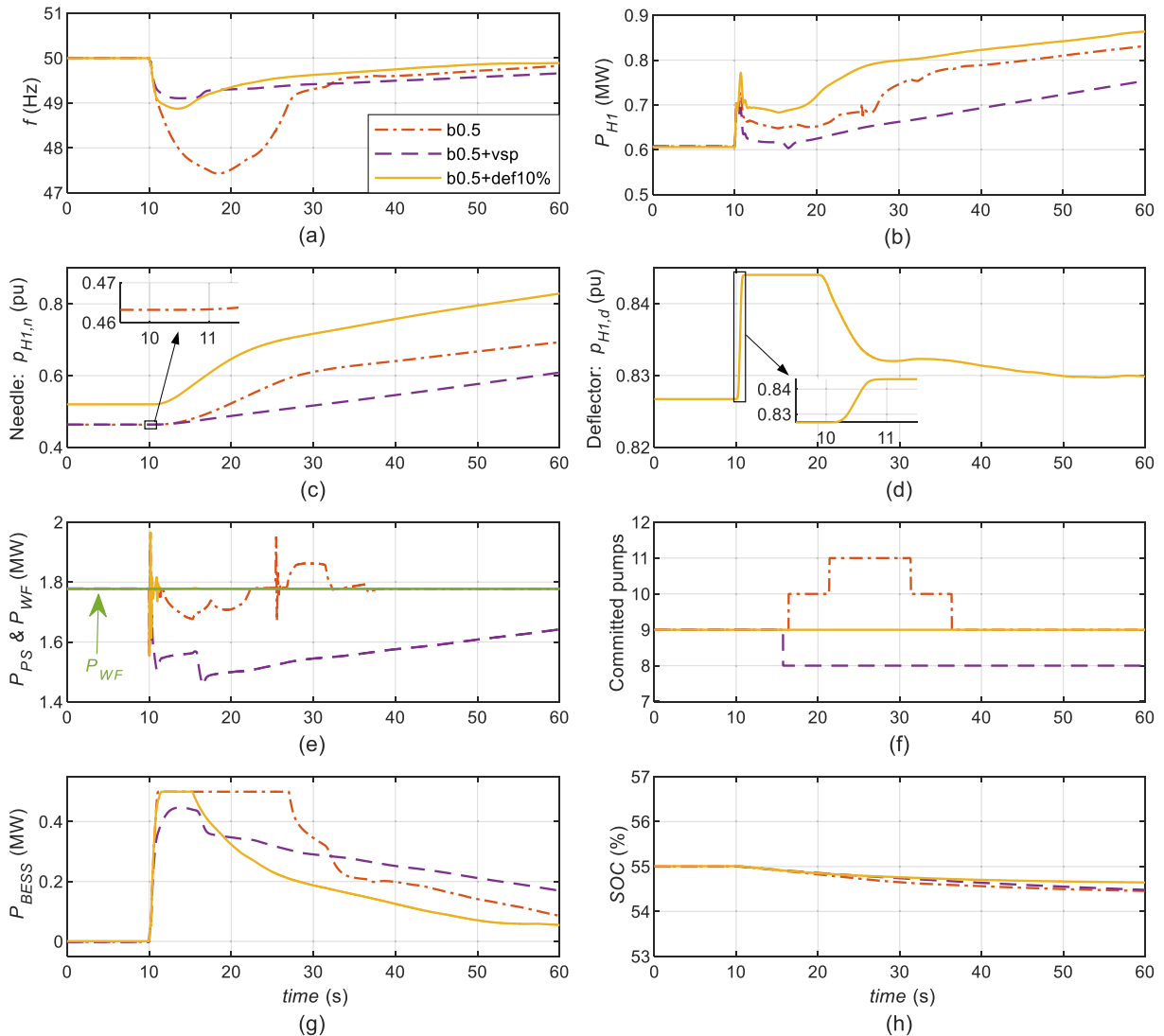
FIGURE 6. System response following a hydroelectric unit (H3) tripping at 10 s, for 3 scenarios with a 0.5 MW BESS. (a) Frequency, (b) hydroelectric unit 1 (H1) active power, (c) H1 needle position, (d) H1 deflector position, (e) pumping station and wind farm active power, (f) number of pumps committed, (g) BESS active power, (h) BESS state of charge.

actively providing reserves. For this reason, similar frequency quality metrics are obtained with deflector and WF control.[3]

To remove the limitations in primary reserves deployed by the WF due to the pumping facility reaction, the option of de-activating the second-by-second wind power tracking functionality of the pumping station is also examined. This is achieved by increasing the filter time constant $T_{w,f}$ shown in Fig. 4 from 0.05 s to 30 s, in order for the pumping facility to track only a slow moving average of the wind power, but not its faster variability. However, it is observed that frequency quality is not improved ($\sigma_f = 0.37$ Hz, $t_{out \pm 0.2Hz} = 54\%$ for $b0.5+vsp+wf17\%$), since this scheme is not taking

full advantage of the regulating capabilities of the pumping station, while the 17% WF power margin cannot make up for the sacrificed pumping station contribution to countering wind power fluctuations.

The ineffective primary reserves provision by the WF, when combined with wind farm tracking by the pumping facility,[4] is also confirmed for the contingency examined in Subsection B. Fig. 8 presents simulation results following the loss of hydro unit H3, with a 0.5 MW BESS, while an equal amount of primary reserves (0.2 MW) are retained by (a) the two remaining hydroelectric units, ($b0.5+def10\%$), (b) the WF ($b0.5+wf11\%$). Although the WF is rapidly deploying reserves ($\sim$0.3 s), the pumping facility also increases

---

[3]Scenarios with σ_f lower for deflector control: *def10%, vsp+def10%, b0.5(wft)+def10%*. Scenarios with σ_f lower for WF control: *b0.5+wf17%, b0.5+vsp+wf17%*.

[4]Results for time periods with significantly less wind turbulence (not shown), also support this statement.

TABLE 3. Key performance indices of deflector and wind farm frequency control, at high wind volatility Conditions: frequency maximum (f_{max}), minimum (f_{min}) & standard deviation (σ_f) and time outside the 49.8-50.2 Hz window ($t_{out} \pm 0.2$Hz).

No	Scenario	BESS rated power (MW)	VSP droop control	BESS wind farm tracking	Wind farm reserve (%)	Deflector reserve (%)	f_{max} (Hz)	f_{min} (Hz)	σ_f (Hz)	$t_{out\pm0.2Hz}$ (%)
1	def10%	-	no	-	-	10	51.5	<48	0.94	75
2	wf17%	-	no	-	17	-	51.6	<48	1.67	89
3	vsp+def10%	-	yes	-	-	10	51.4	<48	0.84	73
4	vsp+wf17%	-	yes	-	17	-	50.9	<48	0.94	70
5	b0.5+def10%	0.5	no	no	-	10	50.7	48.8	0.40	51
6	b0.5+wf17%	0.5	no	no	17	-	50.5	48.8	0.37	55
7	b0.5(wft)+def10%	0.5	no	yes	-	10	50.5	48.9	0.32	35
8	b0.5(wft)+wf17%	0.5	no	yes	17	-	50.4	48.9	0.34	54
9	b0.5+vsp+def10%	0.5	yes	no	-	10	50.7	48.9	0.36	40
10	b0.5+vsp+wf17%	0.5	yes	no	17	-	50.4	48.9	0.31	39
11	b0.5(wft)+vsp+def10%	0.5	yes	yes	-	10	50.5	49.0	0.28	30
12	b0.5(wft)+vsp+wf17%	0.5	yes	yes	17	-	50.4	48.9	0.28	34
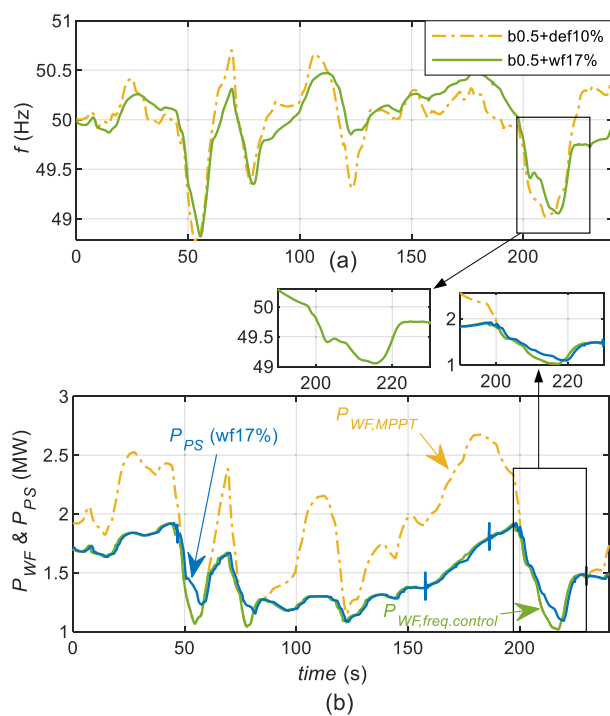
FIGURE 7. System response under high wind fluctuations, for deflector and wind farm frequency control, while having a 0.5 MW BESS on-line. (a) Frequency, (b) wind farm and pumping station active power.

its power absorption due to the WF tracking scheme. The pumping station eventually matches the WF power 12 s after the H3 loss, mainly due to the time delay between successive pumps' switchings.

As a conclusion, although the mechanical deflector control system is slower than the power control of inverter-interfaced WTs, the former leads to superior performance, because the WF cannot provide reserves when needed if the pumping facility tracks its output.

D. COMMUNICATION DELAY SENSITIVITY ANALYSIS

The robustness of the HPS control against communication system delays is evaluated, for latencies in the range of 0.2 to
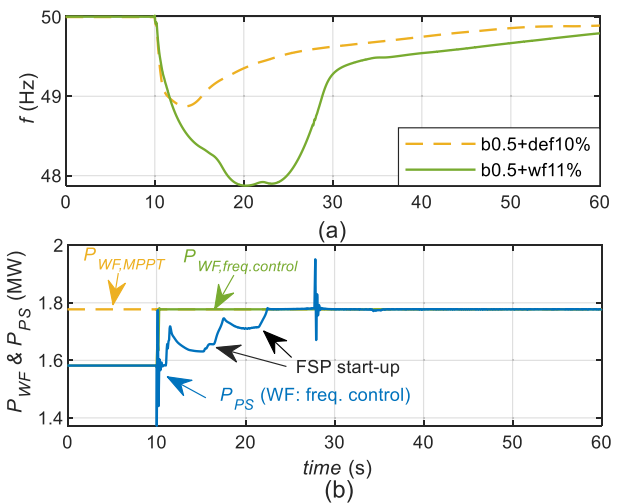

FIGURE 8. System response following a hydroelectric unit (H3) tripping at 10 s, for deflector and wind farm frequency control, in the presence of a 0.5 MW BESS. (a) Frequency, (b) wind farm and pumping station active power.

5 s,[5] although lags exceeding 1 s are not expected [57], [58]. Scenarios with a 1 MW BESS and VSPs with droop control are examined for the conditions of Subsection A, with and without the BESS WFT scheme. Table 4 includes the KPIs for all different cases, whereas Fig. 9 presents the frequency response when activating the wind farm-tracking scheme for the BESS.

As expected, higher time delays lead to worse frequency quality. Comparing scenarios with the same time lag in Table 4, benefits from activating BESS WFT decrease as the latency increases. A 5-s delay seems to be a turning point for the effectiveness of BESS WFT, as similar KPIs are observed with and without activating this functionality.

---

[5]Communication delays between the WF and the pumping station are assumed equal to the delays between pumping station and BESS ($T_{wp,d} = T_{pb,d}$).
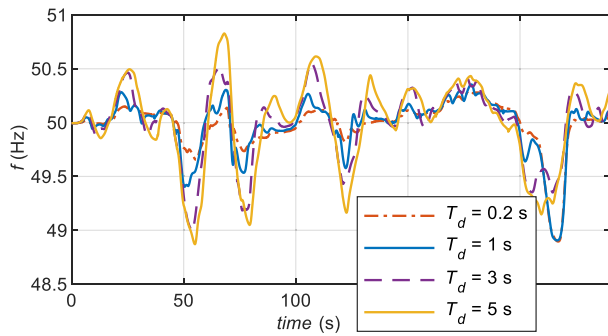
FIGURE 9. Frequency response under high wind fluctuation conditions for time delay sensitivity analysis, with a 1 MW BESS on-line in wind farm tracking and VSP droop control.

TABLE 4. Key performance indices for various wind farm-pumping station ($T_{wp,d}$) and pumping station-battery system ($T_{pb,d}$) time delays, with A 1-MW bess and vsp droop control, at high wind volatility conditions.

BESS WFT	$T_{wp,d} = T_{pb,d}$ (s)	f_{max} (Hz)	f_{min} (Hz)	σ_f (Hz)	$t_{out\pm0.2Hz}$ (%)	ET_b (kWh)
	0.2	50.6	49.0	0.36	44	17.0
Off	1	50.6	49.0	0.37	45	17.8
	3	50.6	49.0	0.39	51	19.4
	5	50.7	48.8	0.41	53	20.3
	0.2	50.3	48.9	0.23	18	18.9
On	1	50.4	48.9	0.26	29	19.5
	3	50.6	49.0	0.33	46	20.6
	5	50.8	48.9	0.41	56	21.5

TABLE 5. Wind farm parameters.

Parameter	Symbol	Value
WT rated power	$P_{w,n}$	0.9 MW
Droop coefficient	R_w	0.05
WF measurement filter time constant	$T_{w,f}$	0.05 s
WF-pumping station communication delay	$T_{wp,d}$	1 s

E. DISCUSSION

Without the supplementary frequency control measures examined, the island system cannot cope with challenging real-time operating conditions, without any fast thermal unit in operation. The current study quantifies the positive effect of all examined solutions enhancing the primary frequency response of a PHS-based hybrid station, with the most promising solution being the installation of a BESS. The implementation of the proposed wind-farm-tracking module in the BESS controller will effectively complement the pumping station in tracking the generation of the wind farm under highly variable wind conditions, at the cost of increased BESS energy throughput. Sufficient BESS power rating and fast communication between the pumping facility and BESS significantly enhance the benefits from implementing this control method.

Although inverter-interfaced batteries outperform the mechanical deflector control in terms of frequency regulation capabilities and energy efficiency, the high capital

TABLE 6. Hydroelectric units' parameters.

Parameter	Symbol	Value
Rated power (H1)	$P_{H1,n}$	1.05 MW
Rated power (H2, H3)	$P_{H2-3,n}$	1.55 MW
Needle jet area constant 1	$k_{h,1}$	1.462
Needle jet area constant 2	$k_{h,2}$	−0.462
Wave travel time (H1)	$T_{H1,e}$	3.3 s
Wave travel time (H2, H3)	$T_{H2-3,e}$	0.02 s
Wave travel time (common pipe of H2-H3)	$T_{hc,e}$	2.54 s
Surge impedance (H1)	$Z_{H1,0}$	1.16
Surge impedance (H2, H3)	$Z_{H2-3,0}$	0.72
Surge impedance (common pipe of H2-H3)	$Z_{hc,0}$	0.3
Friction loss coefficient (H1)	f_{H1}	30.8
Friction loss coefficient (H2, H3)	f_{H2-3}	3.87
Friction loss coefficient (common pipe of H2-H3)	f_{hc}	79.2
No-load flow rate (H1)	$q_{H1,nl}$	0.07 m³/s
No-load flow rate (H2, H3)	$q_{H2-3,nl}$	0.035 m³/s
Turbine proportionality factor (H1)	$A_{H1,t}$	1.28
Turbine proportionality factor (H2, H3)	$A_{H2-3,t}$	1.25
Damping factor	D_{H1-3}	1
Inertia constant (H1)	H_{H1}	1.8 s
Inertia constant (H2, H3)	H_{H2-3}	4.4 s
Proportional gain (deflector control: off)	$K_{h,p}$	2
Integral gain (deflector control: off)	$K_{h,i}$	0.1 s⁻¹
Proportional gain (deflector control: on)	$K_{h,p}$	10
Integral gain (deflector control: on)	$K_{h,i}$	0.3 s⁻¹
Pilot servomotor time constant	$T_{h,p}$	0.05 s
Droop coefficient	R_h	0.05
Filter time constant	$T_{h,f}$	0.2 s
Needles' servomotor gain 1	$\alpha_{h,n,1}$	0.6
Needles' servomotor gain 2	$\alpha_{h,n,2}$	0.05
Needles' rate limit	$\left\|\dfrac{dp_{h,n}}{dt}\right\|_{max}$	0.02 pu/s
Servomotor gain	$K_{h,d}$	15
Deflectors' maximum ramping rate	$\left\|\dfrac{dp_{h,d}}{dt}\right\|_{max}$	0.79 pu/s
Deflectors' minimum ramping rate	$\left\|\dfrac{dp_{h,d}}{dt}\right\|_{min}$	−0.5 pu/s

TABLE 7. Pumping station parameters.

Parameter	Symbol	Value
Rated power of pumps	$P_{p,n}$	0.25 MW
Time between pump switchings	$T_{p,on/off}$	5 s
Inertia constant (FSPs)	H_{fsp}	2.1 s
Maximum power (VSPs)	$P_{vsp,max}$	0.25 MW
Minimum power (VSPs)	$P_{vsp,min}$	0.125 MW
VSP measurement filter time constant	$T_{p,f}$	0.05 s
Pump station-BESS communication delay	$T_{pb,d}$	1 s
Droop coefficient (VSPs)	R_p	0.05

TABLE 8. Battery storage parameters.

Parameter	Symbol	Value
Droop coefficient	R_b	0.02
Maximum proportional gain	$K_{b,max}$	0.01
Proportional gain parameter 1	$P_{b,1}$	0.05
Proportional gain parameter 2	$P_{b,2}$	0.10

cost of batteries makes the exploitation of deflector control a viable approach to decrease the necessary BESS capacity. A major limitation is the resulting waste of available hydro energy, to allow for upward power regulation through

deflector control. However, renewable energy rejections are inevitable at very high RES shares [4], [5]. Wasting a fraction of the water available in the upper reservoir will create room for additional stochastic RES energy to be stored, partly compensating for the "hydroelectric energy curtailments". To implement such a deflector control scheme it is necessary to ensure that the mechanical system is designed to withstand the resulting increased wear and tear [33].

The WF cannot be relied upon for the provision of primary reserves, as its contribution is canceled out by the wind power tracking functionality of the pumping facility. Thus, combining WF frequency regulation and WF tracking by the pumping station is not advised. In any case, non-stochastic resources must be available to support frequency regulation under low wind speed conditions.

V. CONCLUSION

In this study, several solutions are examined to support 100% RES penetration in island grids relying on wind power and pumped-hydro storage. In the absence of thermal units, frequency control and stability of such systems becomes a major challenge due to the limitations in hydro unit response associated with the water column dynamics. Ikaria, a small, non-interconnected Greek island, is used as a study case. Taking advantage of available variable speed pumps, the pumping facility tracks the power produced by the wind farm, to limit the negative effect of wind power variability on frequency quality.

One option to improve the response of Pelton turbines is implementing deflector control in normal operation, whereby the water jets are partially deflected away from turbine blades to reduce turbine output without resorting to needle control and therefore being impacted by the dynamics of the water column. Simulation results demonstrate the effectiveness of this scheme, its main drawback being the under-exploitation of available water for electricity production, by wasting its fraction being deflected off the blades, when fast upward regulation (i.e. under-frequency response) is sought from the units. This drawback needs to be evaluated in the context of the high curtailments that inevitably take place in autonomous systems at high RES penetration levels. Frequency support from the wind farm, the second measure examined resulting in RES curtailments, is not effective, as any reserves deployed by the WTs are canceled out by the pumping facility tracking their output power.

Another solution examined is implementing droop control to provide fast frequency response by the inverter-driven variable-speed pumps. The droop placed on the wind-power-tracking reference to the pumps, although effective, it is limited by the narrow power regulation range of the pumps, which is already exploited for wind power tracking purposes.

A fourth option is the installation of batteries to complement pumped hydro in fast regulation tasks, while also improving the wind power tracking capabilities of the hybrid plant under high wind variability conditions. Simulations prove that batteries are the most effective means to successfully manage frequency regulation challenges, while a concurrent application with deflector and variable-speed pump control would probably prove most cost-effective.

Further research topics based on the results presented in this work include:

- Simulating the scheduling process, resulting in varying deflector reserve margin and primary reserves provided by the VSPs throughout the year, while considering the availability of fast reserves from other units (thermal units, BESS), the cost of underexploiting water inflows and the resulting BESS, deflector and VSP wear-and-tear cost.
- Optimal BESS sizing, considering cost and the other flexibility resources available to the system.
- Further explore when implementing frequency regulation by the wind turbines is beneficial to performing wind power tracking by the pumping station.

APPENDIX.
SYSTEM PARAMETERS
See Tables 5–8.

REFERENCES

[1] *World Energy Outlook 2022*, Int. Energy Agency (IEA), Paris, France, 2022.

[2] *Maximising Social Welfare of Energy Storage Facilities Through Multi-Service Business Cases*, Eur. Assoc. Storage Energy (EASE), Brussels, Belgium, 2019.

[3] C. Breyer et al., "On the history and future of 100% renewable energy systems research," *IEEE Access*, vol. 10, pp. 78176–78218, 2022.

[4] G. N. Psarros and S. A. Papathanassiou, "Electricity storage requirements to support the transition towards high renewable penetration levels—Application to the Greek power system," *J. Energy Storage*, vol. 55, Nov. 2022, Art. no. 105748.

[5] G. N. Psarros, E. G. Karamanou, and S. A. Papathanassiou, "Feasibility analysis of centralized storage facilities in isolated grids," *IEEE Trans. Sustain. Energy*, vol. 9, no. 4, pp. 1822–1832, Oct. 2018.

[6] S. Ntomalis, P. Iliadis, K. Atsonios, A. Nesiadis, N. Nikolopoulos, and P. Grammelis, "Dynamic modeling and simulation of non-interconnected systems under high-RES penetration: The Madeira island case," *Energies*, vol. 13, no. 21, p. 5786, Nov. 2020.

[7] A. G. Papakonstantinou and S. A. Papathanassiou, "Battery energy storage participation in automatic generation control of island systems, coordinated with state of charge regulation," *Appl. Sci.*, vol. 12, no. 2, p. 596, Jan. 2022.

[8] G. N. Psarros, A. G. Papakonstantinou, S. A. Papathanassiou, J. S. Anagnostopoulos, and N. G. Boulaxis, "Contribution of energy storage to capacity adequacy—Application to island power systems," in *Proc. 48th CIGRE Session*, 2020, pp. 1–11.

[9] P. A. Dratsas, G. N. Psarros, and S. A. Papathanassiou, "Battery energy storage contribution to system adequacy," *Energies*, vol. 14, no. 16, p. 5146, Aug. 2021.

[10] P. A. Dratsas, G. N. Psarros, S. A. Papathanassiou, D. Evagorou, A. Frixou, and A. Poullikkas, "Mid-term electricity storage needs of the power system of Cyprus," in *Proc. 49th CIGRE Session*, 2022, pp. 1–10.

[11] P. A. Dratsas, G. N. Psarros, and S. A. Papathanassiou, "Capacity value of pumped-hydro energy storage," in *Proc. 2nd Int. Conf. Energy Transition Medit. Area (SyNERGY MED)*, Oct. 2022, pp. 1–6.

[12] M. A. Bidgoli, W. Yang, and A. Ahmadian, "DFIM versus synchronous machine for variable speed pumped storage hydropower plants: A comparative evaluation of technical performance," *Renew. Energy*, vol. 159, pp. 72–86, Oct. 2020.

[13] Y. Deng, P. Wang, A. Morabito, W. Feng, A. Mahmud, D. Chen, and P. Hendrick, "Dynamic analysis of variable-speed pumped storage plants for mitigating effects of excess wind power generation," *Int. J. Electr. Power Energy Syst.*, vol. 135, Feb. 2022, Art. no. 107453.

[14] W. Yang and J. Yang, "Advantage of variable-speed pumped storage plants for mitigating wind power variations: Integrated modelling and performance assessment," *Appl. Energy*, vol. 237, pp. 720–732, Mar. 2019.

[15] B. Xu, H. Li, P. E. Campana, B. Hredzak, and D. Chen, "Dynamic regulation reliability of a pumped-storage power generating system: Effects of wind power injection," *Energy Convers. Manage.*, vol. 222, Oct. 2020, Art. no. 113226.

[16] S. V. Papaefthymiou, V. G. Lakiotis, I. D. Margaris, and S. A. Papathanassiou, "Dynamic analysis of island systems with wind-pumped-storage hybrid power stations," *Renew. Energy*, vol. 74, pp. 544–554, Feb. 2015.

[17] S. V. Papaefthymiou, "Contribution to the analysis of hybrid wind-hydro-pumped power stations," Ph.D. dissertation, Nat. Tech. Univ. Athens (NTUA), Athens, Greece, 2012.

[18] *Innovative Pumped Storage Hydropower Configurations and Uses*, Capabilities, Int. Forum Pumped Storage Hydropower, 2021.

[19] K. R. Vasudevan, V. K. Ramachandaramurthy, G. Venugopal, J. B. Ekanayake, and S. K. Tiong, "Variable speed pumped hydro storage: A review of converters, controls and energy management strategies," *Renew. Sustain. Energy Rev.*, vol. 135, Jan. 2021, Art. no. 110156.

[20] J. A. Suul, K. Uhlen, and T. Undeland, "Wind power integration in isolated grids enabled by variable speed pumped storage hydropower plant," in *Proc. IEEE Int. Conf. Sustain. Energy Technol.*, Nov. 2008, pp. 399–404.

[21] M. Han, G. T. Bitew, S. A. Mekonnen, and W. Yan, "Wind power fluctuation compensation by variable speed pumped storage plants in grid integrated system: Frequency spectrum analysis," *CSEE J. Power Energy Syst.*, vol. 7, no. 2, pp. 381–395, Mar. 2021.

[22] F. Collier and L. Wozniak, "Control synthesis for an impulse turbine: The Bradley Lake project," *IEEE Trans. Energy Convers.*, vol. 6, no. 4, pp. 639–646, Dec. 1991.

[23] J. Sarasúa, G. Martínez-Lucas, C. Platero, and J. Sánchez-Fernández, "Dual frequency regulation in pumping mode in a wind–hydro isolated system," *Energies*, vol. 11, no. 11, p. 2865, Oct. 2018.

[24] J. I. Sarasúa, G. Martínez-Lucas, and M. Lafoz, "Analysis of alternative frequency control schemes for increasing renewable energy penetration in El Hierro island power system," *Int. J. Electr. Power Energy Syst.*, vol. 113, pp. 807–823, Dec. 2019.

[25] J. I. Sarasúa, G. Martínez-Lucas, H. García-Pereira, G. Navarro-Soriano, Á. Molina-García, and A. Fernández-Guillamón, "Hybrid frequency control strategies based on hydro-power, wind, and energy storage systems: Application to 100% renewable scenarios," *IET Renew. Power Gener.*, vol. 16, no. 6, pp. 1107–1120, Apr. 2022.

[26] H. García-Pereira, M. Blanco, G. Martínez-Lucas, J. I. Pérez-Díaz, and J.-I. Sarasúa, "Comparison and influence of flywheels energy storage system control schemes in the frequency regulation of isolated power systems," *IEEE Access*, vol. 10, pp. 37892–37911, 2022.

[27] J. I. Sarasúa, G. Martínez-Lucas, J. I. Pérez-Díaz, and D. Fernández-Muñoz, "Alternative operating modes to reduce the load shedding in the power system of el Hierro island," *Int. J. Electr. Power Energy Syst.*, vol. 128, Jun. 2021, Art. no. 106755.

[28] N. Masood, R. Yan, T. K. Saha, and S. Bartlett, "Post-retirement utilisation of synchronous generators to enhance security performances in a wind dominated power system," *IET Gener., Transmiss. Distrib.*, vol. 10, no. 13, pp. 3314–3321, Oct. 2016.

[29] I. D. Margaris, S. A. Papathanassiou, N. D. Hatziargyriou, A. D. Hansen, and P. Sorensen, "Frequency control in autonomous power systems with high wind power penetration," *IEEE Trans. Sustain. Energy*, vol. 3, no. 2, pp. 189–199, Apr. 2012.

[30] J. Ouyang, M. Pang, M. Li, D. Zheng, T. Tang, and W. Wang, "Frequency control method based on the dynamic deloading of DFIGs for power systems with high-proportion wind energy," *Int. J. Electr. Power Energy Syst.*, vol. 128, Jun. 2021, Art. no. 106764.

[31] K. V. Vidyanandan and N. Senroy, "Primary frequency regulation by deloaded wind turbines using variable droop," *IEEE Trans. Power Syst.*, vol. 28, no. 2, pp. 837–846, May 2013.

[32] Z. Wu, W. Gao, T. Gao, W. Yan, H. Zhang, S. Yan, and X. Wang, "State-of-the-art review on frequency response of wind power plants in power systems," *J. Mod. Power Syst. Clean Energy*, vol. 6, no. 1, pp. 1–16, Jan. 2018.

[33] *IEEE Guide for the Application of Turbine Governing Systems for Hydroelectric Generating Units*, IEEE Standard 1207-2011 (Revision to IEEE Standard 1207-2004), 2011, pp. 1–139.

[34] L. Wang, J. Zhao, D. Liu, J. Wang, G. Chen, W. Sun, T. Zhao, Y. Zhao, and X. Qi, "Governor tuning and digital deflector control of Pelton turbine with multiple needles for power system studies," *IET Gener., Transmiss. Distrib.*, vol. 11, no. 13, pp. 3278–3286, Sep. 2017.

[35] R. M. Johnson, J. H. Chow, and M. V. Dillon, "Pelton turbine deflector overspeed control for a small power system," *IEEE Trans. Power Syst.*, vol. 19, no. 2, pp. 1032–1037, May 2004.

[36] M. Guezgouz, J. Jurasz, B. Bekkouche, T. Ma, M. S. Javed, and A. Kies, "Optimal hybrid pumped hydro-battery storage scheme for off-grid renewable energy systems," *Energy Convers. Manage.*, vol. 199, Nov. 2019, Art. no. 112046.

[37] *Reports of Power Production in Greek Non-Interconnected Islands*, Hellenic Electr. Distrib. Netw. Operator (HEDNO), Athens, Greece, 2022.

[38] *Non-Interconnected Island Power Systems (NIIs) Management Code (in Greek)*, Hellenic Electr. Distrib. Netw. Operator (HEDNO), Athens, Greece, 2022.

[39] S. V. Papaefthymiou, E. G. Karamanou, S. A. Papathanassiou, and M. P. Papadopoulos, "A wind-hydro-pumped storage station leading to high RES penetration in the autonomous island system of Ikaria," *IEEE Trans. Sustain. Energy*, vol. 1, no. 3, pp. 163–172, Oct. 2010.

[40] S. V. Papaefthymiou and S. A. Papathanassiou, "Optimum sizing of wind-pumped-storage hybrid power stations in island systems," *Renew. Energy*, vol. 64, pp. 187–196, Apr. 2014.

[41] P. Theodoropoulos, A. Zervos, and G. Betzios, "Hybrid systems using pump-storage implementation in Ikaria island," in *Proc. Org. Promotion Energy Technol. Conf. (OPET)*, 2001, pp. 1–4.

[42] G. N. Psarros and S. A. Papathanassiou, "Internal dispatch for RES-storage hybrid power stations in isolated grids," *Renew. Energy*, vol. 147, pp. 2141–2150, Mar. 2020.

[43] S. Papaefthimiou, E. Karamanou, S. Papathanassiou, and M. Papadopoulos, "Operating policies for wind-pumped storage hybrid power stations in island grids," *IET Renew. Power Gener.*, vol. 3, no. 3, pp. 293–307, 2009.

[44] S. Heier, *Grid Integration of Wind Energy: Onshore and Offshore Conversion Systems*, 3rd ed. Hoboken, NJ, USA: Wiley, 2014.

[45] T. Ackermann, *Wind Power in Power Systems*, 2nd ed. West Sussex, U.K.: Wiley, 2012.

[46] I. Erlich and M. Wilch, "Primary frequency control by wind turbines," in *Proc. IEEE PES Gen. Meeting*, Jul. 2010, pp. 1–8.

[47] M. Chinchilla, S. Arnaltes, and J. C. Burgos, "Control of permanent-magnet generators applied to variable-speed wind-energy systems connected to the grid," *IEEE Trans. Energy Convers.*, vol. 21, no. 1, pp. 130–135, Mar. 2006.

[48] V. Yaramasu, A. Dekka, M. J. Durán, S. Kouro, and B. Wu, "PMSG-based wind energy conversion systems: Survey on power converters and controls," *IET Electr. Power Appl.*, vol. 11, no. 6, pp. 956–968, Jul. 2017.

[49] Z. Wu, W. Gao, J. Wang, and S. Gu, "A coordinated primary frequency regulation from permanent magnet synchronous wind turbine generation," in *Proc. IEEE Power Electron. Mach. Wind Appl.*, Jul. 2012, pp. 1–6.

[50] R. G. de Almeida and J. A. P. Lopes, "Participation of doubly fed induction wind generators in system frequency regulation," *IEEE Trans. Power Syst.*, vol. 22, no. 3, pp. 944–950, Aug. 2007.

[51] A. Yazdani and R. Iravani, *Voltage-Sourced Converters in Power Systems: Modeling, Control, and Applications*. Hoboken, NJ, USA: Wiley, 2010.

[52] P. Kundur, *Power System Stability and Control*. New York, NY, USA: McGraw-Hill, 1994.

[53] Working Group Prime Mover and Energy Supply, "Hydraulic turbine and turbine control models for system dynamic studies," *IEEE Trans. Power Syst.*, vol. 7, no. 1, pp. 167–179, Feb. 1992.

[54] J. I. Pérez-Díaz, J. I. Sarasúa, and J. R. Wilhelmi, "Contribution of a hydraulic short-circuit pumped-storage power plant to the load–frequency regulation of an isolated power system," *Int. J. Electr. Power Energy Syst.*, vol. 62, pp. 199–211, Nov. 2014.

[55] S. Hagihara, H. Yokota, K. Goda, and K. Isobe, "Stability of a hydraulic turbine generating unit controlled by P.I.D. governor," *IEEE Trans. Power App. Syst.*, vol. PAS-98, no. 6, pp. 2294–2298, Nov. 1979.

[56] J. Liang and R. G. Harley, "Pumped storage hydro-plant models for system transient and long-term dynamic studies," in *Proc. IEEE PES Gen. Meeting*, Jul. 2010, pp. 1–8.

[57] B. Chaudhuri, R. Majumder, and B. C. Pal, "Wide-area measurement-based stabilizing control of power system considering signal transmission delay," *IEEE Trans. Power Syst.*, vol. 19, no. 4, pp. 1971–1979, Nov. 2004.

[58] H. Wu, K. S. Tsakalis, and G. T. Heydt, "Evaluation of time delay effects to wide-area power system stabilizer design," *IEEE Trans. Power Syst.*, vol. 19, no. 4, pp. 1935–1941, Nov. 2004.

[59] O. Tremblay and L.-A. Dessaint, "Experimental validation of a battery dynamic model for EV applications," *World Electr. Vehicle J.*, vol. 3, no. 2, pp. 289–298, Jun. 2009.

APOSTOLOS I. KONSTANTEAS received the Diploma degree in electrical and computer engineering from the National Technical University of Athens (NTUA), Greece, in 2021. His research interests include renewable energy sources and energy storage.

APOSTOLOS G. PAPAKONSTANTINOU (Member, IEEE) received the Diploma and M.Sc. degrees in electrical engineering from the National Technical University of Athens (NTUA), Greece, in 2013 and 2016, respectively, where he is currently pursuing the Ph.D. degree.

He has worked for the system operator of Greek non-interconnected islands (HEDNO) in the management and development of electricity production and for the Hellenic energy exchange in the operation of spot electricity markets in Greece. His research interests include electricity storage and renewable energy. He is a member of CIGRE.

STAVROS A. PAPATHANASSIOU (Senior Member, IEEE) received the Diploma degree in electrical engineering and the Ph.D. degree from the National Technical University of Athens (NTUA), Athens, Greece, in 1991 and 1997, respectively.

Since 2002, he has been a Professor with the Electric Power Division, NTUA. His research interests include renewable generation, storage, and distributed energy resources, including their grid and market integration. He has worked for the Greek DSO. He has been a member of the Executive Board of the Greek TSO and Market Operator and he is collaborating with the industry in Greece and abroad in RES and storage projects.

● ● ●